

2-1-2009

Evaluation of Live-Load Lateral Flange Bending Distribution for a Horizontally Curved I-Girder Bridge

David S. DePolo
U.S. Army Corps. Of Engineers

Daniel G. Linzell
Pennsylvania State University, dlinzell@unl.edu

Follow this and additional works at: <https://digitalcommons.unl.edu/civilengfacpub>

DePolo, David S. and Linzell, Daniel G., "Evaluation of Live-Load Lateral Flange Bending Distribution for a Horizontally Curved I-Girder Bridge" (2009). *Civil Engineering Faculty Publications*. 152.
<https://digitalcommons.unl.edu/civilengfacpub/152>

This Article is brought to you for free and open access by the Civil Engineering at DigitalCommons@University of Nebraska - Lincoln. It has been accepted for inclusion in Civil Engineering Faculty Publications by an authorized administrator of DigitalCommons@University of Nebraska - Lincoln.

Evaluation of Live-Load Lateral Flange Bending Distribution for a Horizontally Curved I-Girder Bridge

David S. DePolo¹ and Daniel G. Linzell²

Abstract: This paper focuses on levels of live-load lateral bending moment (bimoment) distribution in a horizontally curved steel I-girder bridge. Work centered primarily on the examination of (1) data from field testing of an in-service horizontally curved steel I-girder bridge and (2) results from a three-dimensional numerical model. Experimental data sets were used for calibration of the numerical model and the calibrated model was then used to examine the accuracy of lateral bending distribution factor equations presented in the 1993 Edition of the (AASHTO) *Guide Specifications for Horizontally Curved Bridges*. It is of interest to examine these equations for potential use in preliminary design even though they have been eliminated during recent AASHTO specification modifications that addressed curved bridge analysis, the 2005 Interims to the AASHTO *LRFD Bridge Design Specifications*. In addition, they were developed using idealized computer models and small-scale laboratory testing with very few field tests of in-service full-scale curved steel bridges conducted to support or refute their use. Results from such experimental and numerical studies are presented and discussed herein.

DOI: 10.1061/(ASCE)1084-0702(2008)13:5(501)

CE Database subject headings: Live-load; Bending; Bridges; Curvature; Bridges, girder; Load distribution; Numerical models.

Introduction

Equations for predicting levels of lateral bending (bimoment) distribution in curved I-girder bridges are provided in the *AASHTO Guide Specifications for Horizontally Curved Highway Bridges* (AASHTO 1993). Lateral bending distribution factors (LBDFs) given in the 1993 AASHTO guide Specifications account for warping effects but are based on idealized computer models, small-scale testing, and mathematical approximations that attempt to mimic actual behavior of the structure. However, they have not been verified against field data and have not been included in any subsequent curved girder specifications, including modifications to curved girder analysis requirements in the 2005 interims to the *AASHTO LRFD Bridge Design Specifications* (AASHTO 2005), and are no longer suggested for use. Reasons for their removal can be attributed to concerns about accuracy, which in part are caused by a lack of verification against actual bridge data, and a shift in analysis approaches for curved structures away from a traditional, line girder approach. The only mention of distribution factors in the 2005 interims for use in a line girder analysis can be found in Article 4.6.1.2.4b and relate solely to determination of major-axis bending moments (typically, moments that result in vertical deflection of the structure) and shears. This paper states that curvature effects on vertical bending moments can be ignored if specific conditions are met. If these conditions are met, a line

girder analysis may be performed for an equivalent straight girder using straight girder live-load distribution factors, where S = girder spacing in feet. The Commentary to this paper indicates that approximations for curvature effects in all curved I-girders should occur, with lateral bending moments being calculated using approximate approaches from the literature developed in association with research related to the V-load method (USS 1984).

As a result of the removal of the LBDF equations from the 2005 AASHTO interims and additional recommendations given in Article 4.6.1.2.1 of the interims for analysis of steel structures curved in plan, stating that all analyses, including the first preliminary analysis, be based on rational methods and include integrated behavior of structural components, designers have been using other methods to complete the analysis and design process. These methods, which can include the V-load method and three-dimensional finite-element models using commercially available software programs, typically, are more time consuming for a preliminary analysis where initial distribution of the vertical and lateral bending moments is established. Although the V-load method is certainly suitable for preliminary analysis, it is not a line girder analysis in the traditional sense since the entire superstructure is considered when calculating the V loads and still requires a fair amount of effort to estimate these curvature effects. In addition, because it is an approximate method, once preliminary estimates have been made a detailed analysis may still be necessary depending on the complexity of the structure. Therefore, interest exists in examining and assessing the accuracy of the LBDFs presented in the 1993 AASHTO guide specifications due to their potential for use during an initial, traditional, line girder analysis that can serve as a preliminary iteration for the entire design process. This paper will focus on evaluating the accuracy of these live-load factors for lateral bending by comparing their predictions to calibrated numerical data.

¹Structural Engineer, GS11, U.S. Army Corps. Of Engineers, Sacramento, CA 95815.

²Associate Professor, Dept. of Civil and Environmental Engineering, The Pennsylvania State Univ., University Park, PA 16802.

Note. Discussion open until February 1, 2009. Separate discussions must be submitted for individual papers. The manuscript for this paper was submitted for review and possible publication on December 5, 2006; approved on January 9, 2008. This paper is part of the *Journal of Bridge Engineering*, Vol. 13, No. 5, September 1, 2008. ©ASCE, ISSN 1084-0702/2008/5-501-510/\$25.00.

Background

Since the mid-1800s, researchers from around the world have been conducting studies on curved beams. A large portion of recent documented curved steel beam research in the United States stemmed from a collaborative effort by a group known as the Consortium of University Research Teams (CURT). From 1969 until the mid-1970s, the CURT team was responsible for conducting research that culminated with the ASCE and AASHTO publishing a set of design guidelines, the *AASHTO Guide Specifications for Horizontally Curved Bridges* (AASHTO 1980). This development provided engineers with a first set of complete design equations and also helped spur further research to investigate the accuracy and completeness of these specifications. Since the CURT project, there has been a significant amount of experimental and numerical research conducted on the behavior of curved steel I-girder bridges, including some documented field tests (Galambos et al. 1996; Hajjar and Boyer 1997; Krzmarzick and Hajjar 2006; McElwain and Laman 2000). More detailed summaries of these studies are provided elsewhere (Nevling et al. 2006). A large portion of recent, relevant numerical research was credited to the Federal Highway Administration's (FHWA) Curved Steel Bridge Research Program (CSBRP) (Kulicki et al. 2006); however, this work was completed in conjunction with laboratory tests and did not focus on live-load distribution. Most research focusing on lateral bending distribution in curved steel bridges was conducted from 1970 to 1990 by researchers unaffiliated with CSBRP, such as Heins (Heins and Jin 1984), Siminou (Heins and Siminou 1970), and Brockenbrough (Brockenbrough 1986). However, each researcher who developed new equations or modified an existing equation used numerical models to verify their accuracy with limited comparison to actual, full-scale bridge response.

Objectives

The project detailed herein involved examining the behavior of a single, in-service, horizontally curved, steel, I-girder bridge both experimentally and numerically. Field testing and numerical models were used to meet the following objectives: (1) develop validated numerical models using field data; (2) determine live-load distribution factors using various methods described herein; and (3) compare these factors to one another and the field data to

Table 1. Girder Lengths

Girders	Span 1 (L1) [m (ft)]	Span 2 (L2) [m (ft)]	Span 3 (L3) [m (ft)]
G1	23.83 (78.18)	31.56 (103.56)	24.84 (81.50)
G2	23.67 (77.66)	31.15 (102.2)	24.23 (79.49)
G3	23.52 (77.17)	30.77 (102.2)	23.67 (77.66)
G4	23.38 (76.71)	30.42 (99.8)	23.17 (76.02)
G5	23.25 (76.28)	30.10 (98.75)	22.72 (74.54)

evaluate their accuracy for the structure that was tested. Methods used for determination of live-load distribution factors are as follows: (a) an equation provided in the 1993 AASHTO guide specifications for lateral bending distribution; (b) a method described in the 1993 AASHTO guide specifications that utilizes modified distribution factors that represent transverse truck position; and (c) the calibrated numerical model.

Structure Description

The studied bridge is located south of Lewistown, Pa., on State Route 103 in Mifflin County. The bridge is 77.57 m (254 ft, 6 in.) in length and has a radius of curvature of 173.72 m (570 ft) to the center girder. The north and south abutments have skews of 35 and 60°, respectively, relative to the center line of the bearings. The bridge consists of three continuous spans composed of five ASTM A572 (50 ksi) plate girders, spaced at 2.39 m (7.84 ft) center to center. For all five girders top flange plates are 356 mm × 16 mm (14 in. × 0.63 in.) and web plates are 1,219 mm × 13 mm (48 in. × 0.5 in.). Bottom flange plates of G1 and G2 are 356 mm × 25 mm (14 in. × 1 in.) and G3, G4, and G5 are 356 mm × 32 mm (14 in. × 1.25 in.). Girders are intermediately braced using “K” shaped cross frames that consist of two L 3 mm1/2 × 31/2 × 3/8 angles for the diagonals with L31/2 × 31/2 × 3/8 double angles, long legs back to back, for the top and bottom chords. Cross frames at the bearings and over the piers are similar to the intermediate frames, except the top chord is a WT15 × 49.5. Girder lengths are detailed in Table 1 and simplified plan and cross-section drawings are given in Figs. 1 and 2. The elevation view in Fig. 1 details that, along with two vehicular lanes, the studied bridge also has a pedestrian walkway located directly over interior Girder 1.

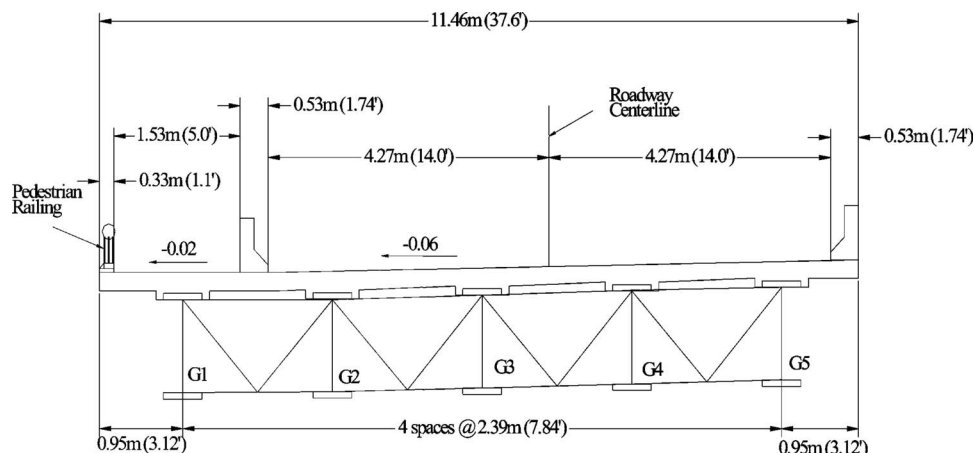


Fig. 1. Lewistown Bridge cross section

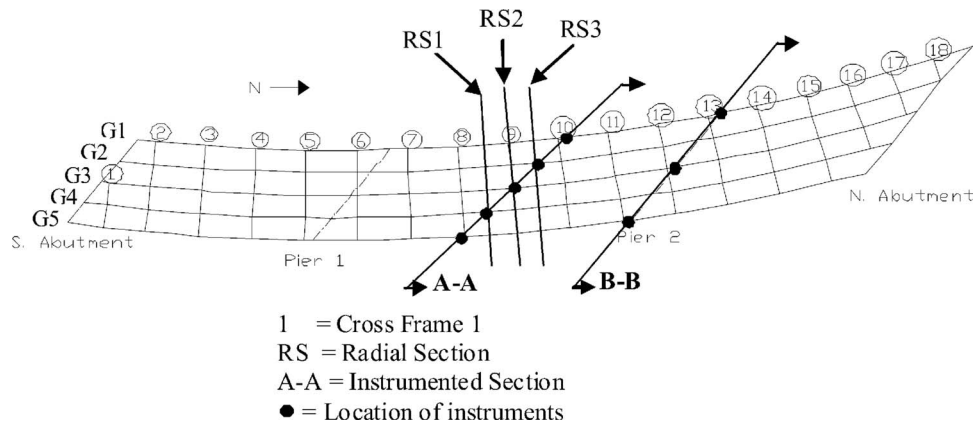


Fig. 2. Plan view of instrument locations

Field Testing

A preliminary grillage analysis of the bridge was conducted to establish instrument locations using SAP2000 (Linzell et al. 2002). Instruments were placed on the bridge at the location of maximum positive and negative vertical bending. Instruments at Section A-A, detailed in Fig. 2, were near the middle of Span 2 in the region of maximum positive vertical bending and at Section B-B above Pier 2 were in the region of maximum negative vertical bending.

For the purpose of this study, eight static tests were examined. A detailed summary of the entire testing procedure is provided elsewhere (Linzell et al. 2002). Tests were conducted using standard fully loaded Pennsylvania Department of Transportation (PennDOT) dump trucks of known weight. Detailed information on the test trucks is given in Table 2; Table 3 details locations of those trucks for each static test. The static tests chosen for this study were at prescribed distances from the eastern parapet so that the test trucks could be placed closest to exterior Girder G5; that is, the girder that experiences the most severe curvature effects. Static tests at measured distances from the western parapet were not selected for this study because the presence of a pedestrian walkway did not allow for the test trucks to be placed close to interior Girder G1 (Fig. 1).

Experimental, AASHTO, and Numerical Live-Load Lateral Bending Distribution Factors

Experimental and Numerical Live-Load Lateral Bending Distribution Factors

Recorded strains from the girder flanges inherently had two components, one from vertical bending and one from lateral bending.

Table 2. Test Truck Data

Truck dimensions	Tri axle	Tandem
Total weight	245 kN (55 k)	169 kN (38 k)
Front axle weight	62 kN (14 k)	53 kN (12 k)
Front to middle axle	4.1 m (13.5 ft)	4.1 m (13.5 ft)
Middle to rear axle	1.3 m (4.3 ft)	N/A
Tire width	0.3 m (1.0 ft)	0.3 m (1.0 ft)
Width between tires	2.4 m (8.0 ft)	2.3 m (7.7 ft)

Note: N/A=not available.

Decoupling these effects was achieved by assuming a linear strain distribution across the flange widths and by using Hooke's law to convert recorded strains into stresses. This required extrapolating recorded stresses measured 29 mm (1.14 in.) from the flange tips to values at the tips. Vertical bending stresses were calculated by averaging the stresses at the flange tips and lateral bending stresses were calculated by subtracting vertical bending stresses from tip stresses. Experimental and numerical live-load lateral bending distribution factors were calculated using Eq. (1). While this equation does not match the typical form for determining distribution factors (DF), which typically are presented as a function of bending moments, its use is acceptable since section properties are constant at a radial bridge cross section

$$DF_i = \frac{\sigma_i}{\sum_{i=1}^n \sigma} \quad (1)$$

AASHTO 1993 Guide Specification Lateral Bending Moments and Distribution Factors

Lateral bending distribution factor equations from Article 1.4 of the 1993 AASHTO guide specifications stem from a mathematical model developed by Bell and Heins (1970) and data obtained from testing of curved bridge models by Heins and Bonakdarpour (1971). From these models, the CURT team developed live-load distribution factor equations for lateral flange bending (bimoment) in each girder (using U.S. Customary units)

Table 3. Studied Tests

Test number	Truck transverse position [m (ft)]	Truck longitudinal position from south end [m (ft)]
Static 1	0.6 (2.0) from east parapet	64.3 (211.0)
Static 2	0.6 (2.0) from east parapet	41.8 (137.0)
Static 3	0.6 (2.0) from east parapet	33.5 (110.0)
Static 7	1.2 (4.0) from east parapet	64.3 (211.0)
Static 8	1.2 (4.0) from east parapet	42.1 (138.0)
Static 9	1.2 (4.0) from east parapet	32.9 (108.0)
Static 13	1.8 (6.0) from east parapet	41.5 (136.0)
Static 14	1.8 (6.0) from east parapet	33.5 (110.0)

$$DF_{Bi} = \frac{S}{5.5} [(0.0008L + 0.13) + (0.0022L^2 - 0.59L + 40)R \times 10^{-4}] \quad (2)$$

Eq. (2) allowed for the analysis of a single, isolated curved girder subjected to a line of wheel loads and accounted for the effects of other girders of the system via the modified $S/5.5$ distribution factor based upon radius (R) and span length (L). Eq. (2) reduces to $S/5.5$ for infinite radii.

The complex nature of analyzing a single curved girder necessitated the development of modification factors that account for curvature to relate single curved girders to an equivalent straight girder. The procedure for completing an equivalent straight girder analysis was presented in Article 1.4 of the 1993 AASHTO guide specifications. Here, live-load lateral bending moments were approximated using equivalent straight girder moments with the distribution factor from Eq. (2) being applied to mimic live-load distribution to a single girder within the system and with an additional modification factor (MF) that accounted for curvature and permitted an equivalent straight girder analysis. These modification factors are presented in Eqs. (3) and (4) (AASHTO 1993)

$$MF = \frac{\text{Curved Single Girder Function}}{\text{Single Straight Girder Maximum Bending Moment}} \quad (3)$$

which yields, for the lateral bending moment

$$MF_{Bi} = \frac{35N \cdot \frac{L}{R} - 15}{0.108L - 1.68} \cdot \frac{L}{R} \quad (4)$$

Lateral flange bending moments could then be calculated for curved girders using the following equation:

$$M = MF_{Bi} \cdot DF_{Bi} \cdot M_s \quad (5)$$

As shown in Eq. (5), the designer would calculate a live-load lateral bending moment for the equivalent straight girder subjected to a line of wheel loads and modify this moment to (a) account for the effects of other girders in the system using Eq. (2); and (b) account for the influence of curvature on the resulting equivalent straight girder moment using Eq. (4).

Modified AASHTO Lateral Bending Distribution Factors

To facilitate comparison between numerical and experimental data, the lateral bending distribution factor presented in Eq. (2) and used in Eq. (5) required some adjustment to accurately represent radial location of the trucks on the tested bridge. Eq. (2), a design-based equation, is purely a function of geometric properties and does not reflect radial truck position. Therefore, modified distribution factors were calculated and used in Eq. (5) so recorded stresses allowed for more direct comparison to numerical data by reflecting radial truck positioning. The procedure for modifying the distribution factors involved modeling the deck as a continuous beam with the five girders acting as supports, similar to the "lever rule," as shown in Fig. 3. This simplified model was analyzed for each radial truck placement (Table 3). Using reactions determined from each support and the total live-load, appropriate distribution factors were determined for each static load case using Eq. (6)

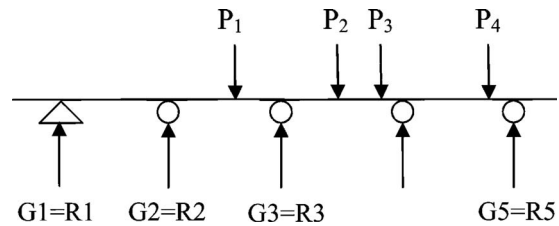


Fig. 3. Continuous beam model for modified AASHTO distribution factors

$$DF_{Bi} = \frac{R_i}{\sum_{i=1}^n P} \quad (6)$$

When substituted into Eq. (5), these distribution factors were used to calculate live-load lateral bending moments for each girder at the locations where numerical and experimental data were obtained. Once live-load lateral bending moments were calculated for each girder, modified LBDFs were calculated using Eq. (1) with live-load lateral bending moments being converted into stresses.

2005 AASHTO Lateral Bending Distribution Factors

The 2005 AASHTO interims no longer contain the equations and methods presented in the 1993 AASHTO guide specifications for determining LBDFs. The only location where a line girder analysis may be acceptable, with distribution factors being incorporated into the line girder analysis, relates to major-axis bending moments and shears and can be found in Article 4.6.1.2.4b. This section states that curvature effects on vertical bending moments can be ignored when the following conditions are met:

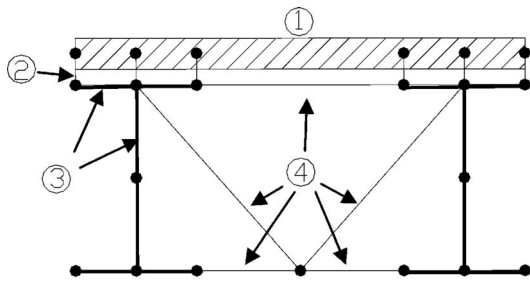
1. Girders are concentric;
2. Bearing lines are not skewed more than 10° from radial;
3. The stiffnesses of the girders are similar; and
4. The arc span divided by the girder radius is less than 0.06 rad.

Here, the arc span, L_{as} , shall be taken as follows:

- L_{as} = girder arc length, simple spans;
- $L_{as} = 0.9 \times$ girder arc length, end spans continuous members; and
- $L_{as} = 0.8 \times$ girder arc length, interior spans continuous members.

If these conditions are satisfied, a line girder analysis may be performed. For a concrete slab on a steel beam bridge an $S/5.5$ distribution factor historically has been used. The *AASHTO LFRD Bridge Design Specifications* (AASHTO 2004) currently use more detailed distribution factor estimation equations from Table 4.6.2.2.2b-1 that account for number of beams, beam spacing, span length, slab thickness, and longitudinal stiffness.

It should be mentioned that the studied bridge does not meet the skew requirement from the aforementioned list. Therefore, according to the AASHTO specifications this bridge cannot be analyzed using a line girder analysis and a more rigorous method would be required. However, it was of interest to compare results from the current study to those from historical distribution factors for straight girders and, as a result, factors calculated using $S/5.5$ were also included in the comparisons.



- 1 = Deck Shells (ABAQUS S4R and S3R)
- 2 = Deck to Flange Links (ABAQUS FRAME 3D)
- 3 = Girder Shells (ABAQUS S4R)
- 4 = Cross frame (ABAQUS B31)

Fig. 4. Construction of numerical model

Numerical Modeling

Numerical distribution factors were calculated from a calibrated model developed in ABAQUS/Standard (HKS 2002). This model was generated to provide an additional method for evaluating distribution factors that could be compared to the values from AASHTO. The model allowed for different regions of the superstructure to be evaluated to examine the live-load lateral bending distribution. Three radially aligned cross sections in the region near the maximum positive vertical bending moment Section A-A and the maximum negative vertical bending moment Section B-B (see Fig. 2) were evaluated numerically. Live-load lateral bending distribution factors were directly calculated from numerical data at these sections using Eq. (1).

The numerical model was created in ABAQUS/Standard using beam, shell, and frame elements (Fig. 4). Model validation involved varying the deck's compressive strength and bridge boundary conditions to determine if more accurate predictions of girder strains were achievable when compared to data from field tests in Table 3.

Available bridge plans did not provide accurate information related to deck compressive strength. Therefore, deck strengths ranging from a nominal design value of 4 ksi (0.28 N/m²) up to 7 ksi (0.48 N/m²) were examined to quantify changes in model accuracy. It was determined that changes in results due to adjustment in deck strengths were not significant and a value of 5 ksi (0.35 N/m²), which provided marginal improvement in the numerical results, was used.

Boundary conditions (see Fig. 5) were also examined to determine if supports at the abutments and piers were creating rotational restraints that affected the behavior of the bridge. Additional rotational restraints were applied to supports along Girder 3, the girder with the most constraints in the actual structure; however, trial analyses produced results that marginally improved the accuracy of the results for some girders while decreasing the accuracy of results for others. The additional restraint did not produce beneficial improvement in numerical results for all of the girders. Therefore, the original boundary conditions were used.

Validation

Fig. 6 illustrates comparisons between experimental and numerical distribution factors at Section A-A located near the largest positive vertical bending moment (note: radial wheel line locations are detailed in Fig. 6). These comparisons represent those used to calibrate the numerical model. Test cases Static 8 and Static 8a refer to multiple field tests for that truck position case and ABAQUS refers to numerical values for the that load case. Fig. 6 contains a schematic denoting the trucks radial wheel line positions and location of the center of gravity (CG) of the test trucks wheels. The representative figure demonstrates that, after completing the aforementioned calibration steps, general load distribution trends were predicted accurately using the numerical model.

Discussion of Results

Selected results from the eight static test cases (Table 3) will be presented herein. Results from the remaining static cases and details on how the calculations were performed are found elsewhere (DePolo 2004). Results are presented through comparisons between live-load LBDFs calculated from: (1) field testing; (2) the numerical model; and (3) previously detailed methods from the *AASHTO Guide Specifications for Horizontally Curved Highway Bridges* (AASHTO 1993). It should be emphasized that load distribution to all girders at a given cross section for the eight static truck tests is presented and examined.

AASHTO Live-Load LBDF Evaluation

Positive Bending

Live-load LBDFs for positive bending from equations in the 1993 AASHTO guide specifications are compared to the calibrated nu-

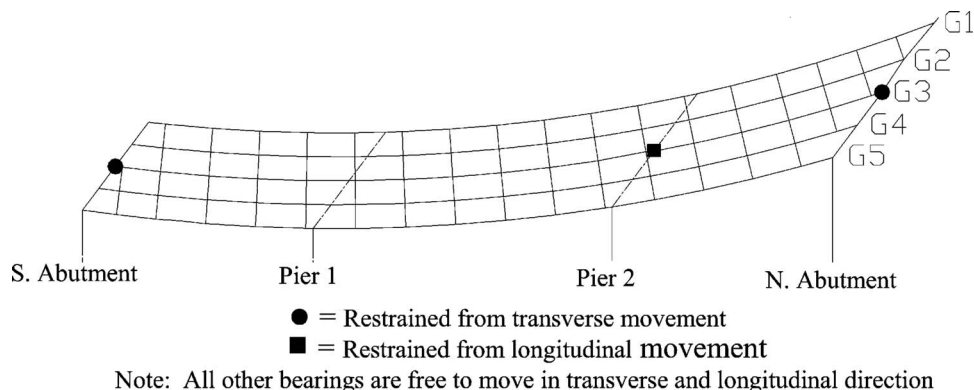


Fig. 5. Boundary conditions for ABAQUS model

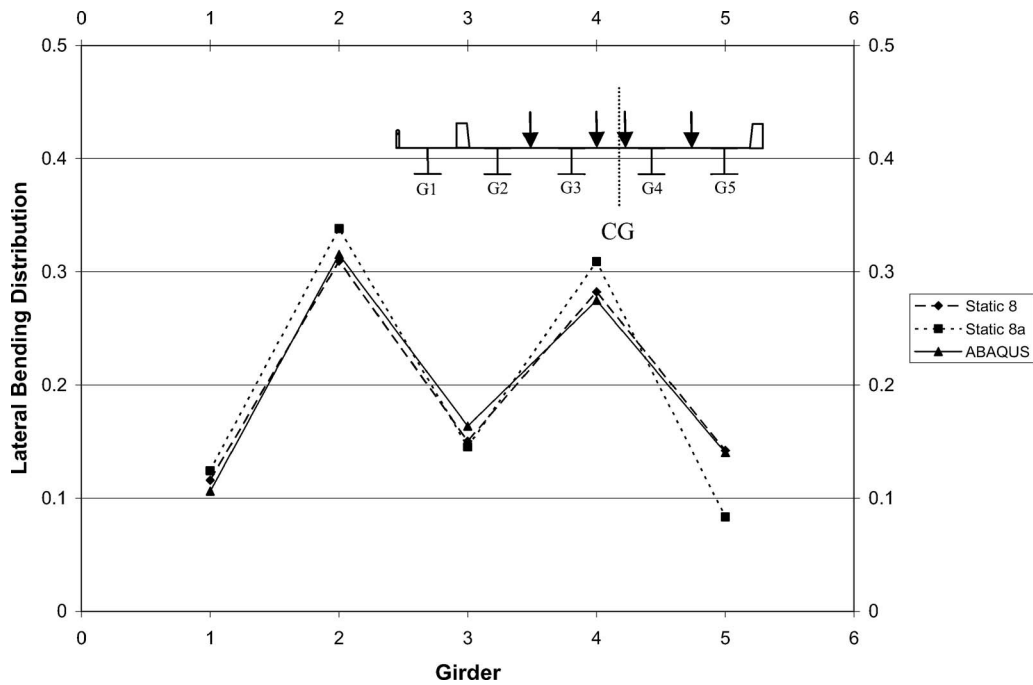


Fig. 6. Live-load lateral bending distribution, static test 8, Section A-A, field versus numerical

merical results. Positive bending distribution factors were calculated for three radially aligned cross sections in Fig. 2. These three radial sections (RS) were located midway between Cross Frames 8 and 9 (RS1), at Cross Frame 9 (RS2), and midway between Cross Frames 9 and 10 (RS3). Distribution factors were calculated at these radial sections as opposed to experimental Section A-A, which was aligned with the skew, to eliminate the influence that changes in lateral bending moment sign and magnitude would have on results near cross-frame locations.

Figs. 7 and 8 illustrate comparisons between numerical and

AASHTO distribution factors at RS1 and RS2 for Static Test 14. Because of the proximity of the three radial cross sections along the span, distribution trends predicted at each cross section did not change significantly, and values for RS3 are not shown here. In Figs. 7 and 8, ABAQUS refers to numerical results, modified AASHTO refers to values calculated using Eq. (6), and AASHTO 1993 refers to factors calculated using LBDP equations in the 1993 guide specifications [Eqs. (2) and (5)].

As shown in Figs. 7 and 8, live-load lateral bending distribution factors calculated using AASHTO equations at the three ra-

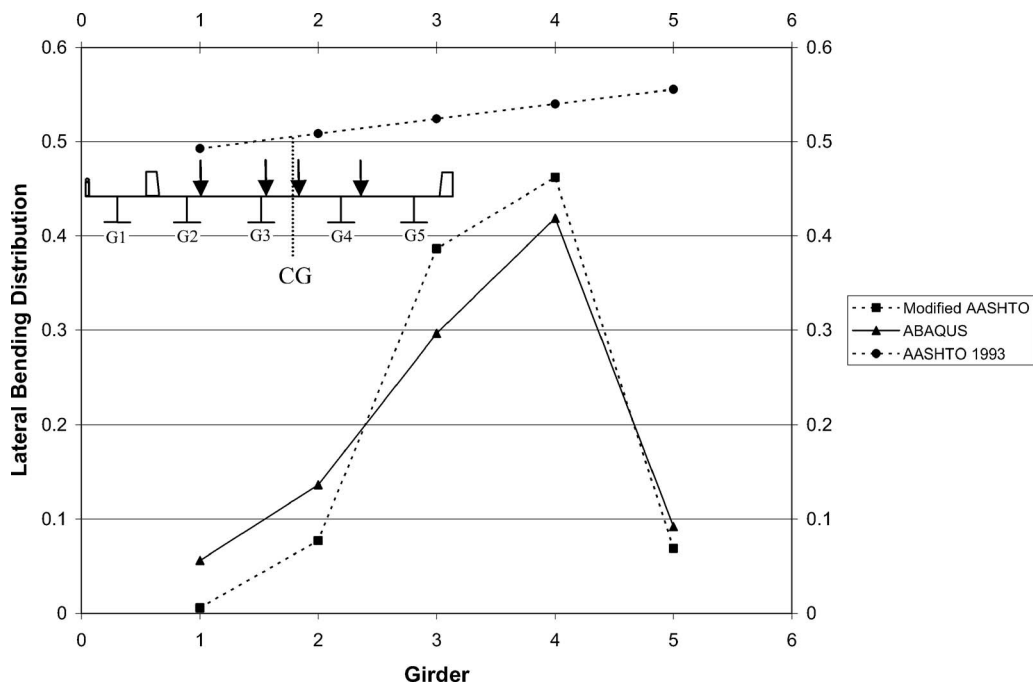


Fig. 7. Static Test 14, Radial Section 1, numerical versus AASHTO

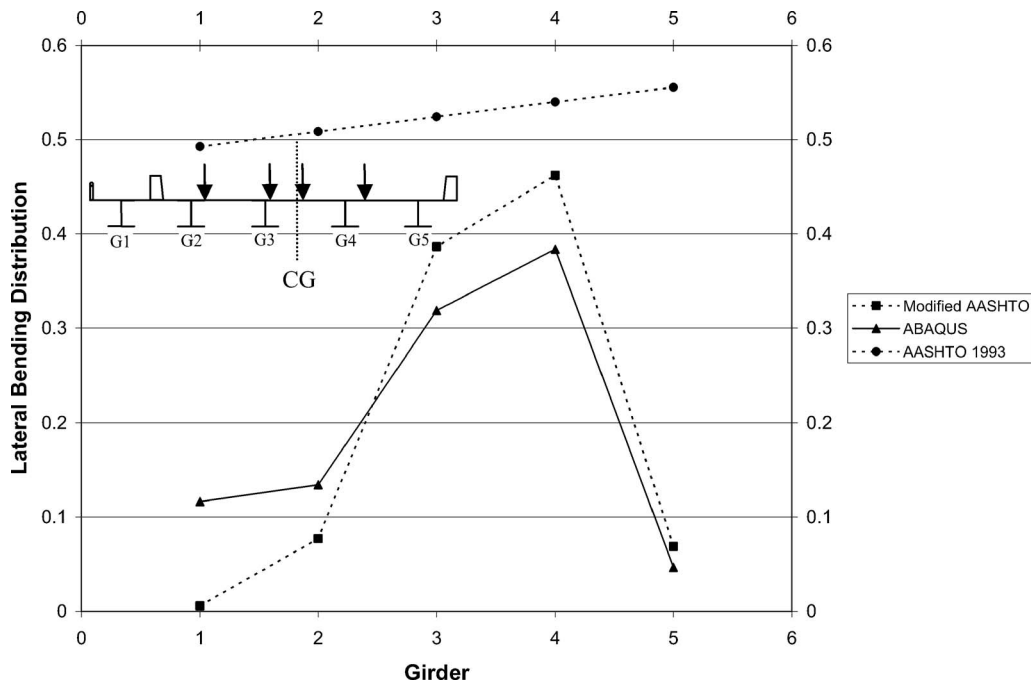


Fig. 8. Static Test 14, Radial Section 2, numerical versus AASHTO

dial cross sections produced conservative values (on the order of 10–30%) for Girders 3 and 4, located near the center of gravity of the test truck wheel lines. In addition, general trends exhibited by the numerical model at the radial sections corresponded fairly well with differences in distribution ranging from 5 to 35% with trends predicted using the modified AASHTO procedure, which adjusted the distribution factor presented in Eq. (2) and used in Eq. (5) to accurately represent the radial location of the test trucks on the tested bridge.

Since designers, typically, are concerned with generating maximum moment effects for sizing girders, it was of interest to compare maximum LBDFs for each girder for the series of tests that were studied. Therefore, numerical distribution factors for RS1, RS2, and RS3 were used to plot maximum distribution factors for the tests listed in Table 3 and were compared to factors in the 1993 AASHTO guide specifications.

Fig. 9 illustrates that maximum distribution factors for each girder determined from the test truck locations from the numerical

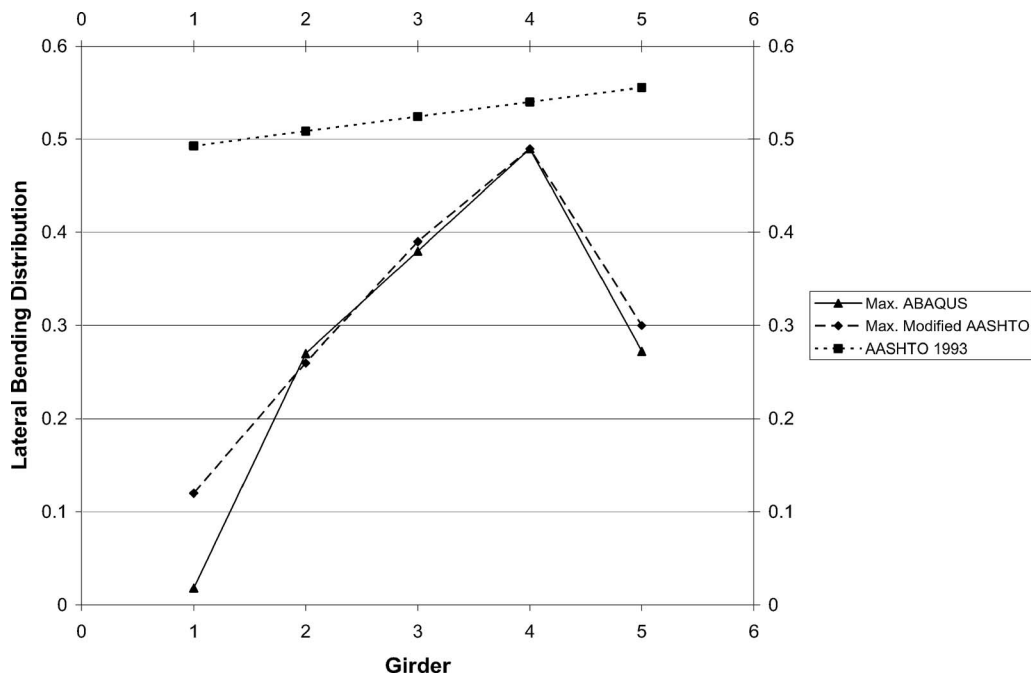


Fig. 9. Maximum live-load lateral bending distribution factors, RS1, RS2, and RS3

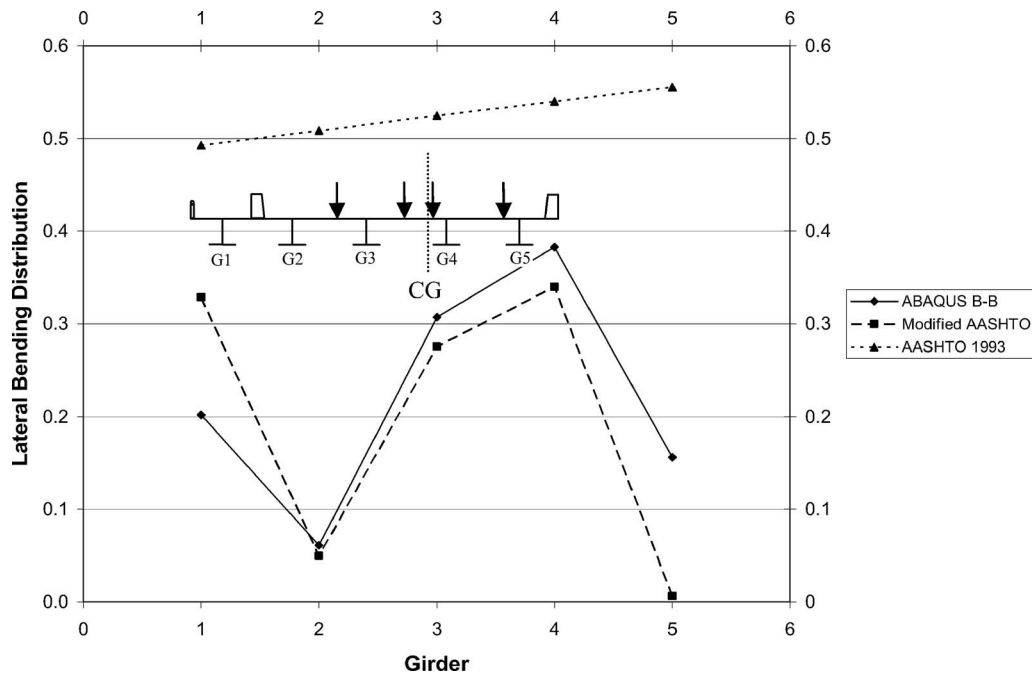


Fig. 10. Live-load lateral bending distribution, static test 3, Section B-B, numerical versus AASHTO

and modified AASHTO results produced a comparable trend. The 1993 AASHTO guide specification LBDFs were conservative for all girders, with levels of conservatism ranging from 8% for Girder 4 to 24% for Girder 1. High levels of conservatism observed for Girders 1, 2, and 5 were attributed to the relative distances of the centers of gravity of the test trucks from those girders.

Negative Bending

Negative bending LBDFs over Pier 2 (Section B-B) were compared against factors determined from the 1993 AASHTO guide specifications. Numerical LBDFs for Section B-B were determined for a section aligned with the bridge skew since, at this location, the pier provided similar restraint to all girders.

Fig. 10 illustrates comparisons between numerical, modified AASHTO, and the 1993 AASHTO guide specification distribution factors for Static Test 3 at Section B-B. ABAQUS B-B refers to numerical tests results; modified AASHTO refers to values calculated using Eq. (6); and AASHTO refers to the factors calculated using the 1993 guide specifications [Eqs. (2) and (5)].

Numerical live-load lateral bending distribution factors predicted for Section B-B showed trends that corresponded well with the modified AASHTO predictions, with results indicating that Girders 3 and 4, the girders closest to the test truck's center of gravity, again had the highest distribution factors. The 1993 AASHTO guide specification LBDFs were still the most conservative for each girder, with levels of conservatism ranging between 25% for Girders 3 and 4 and close to 90% for Girders 1, 2, and 5, which are again located furthest from the centers of gravity of the test trucks.

As with the positive moment region, it was of interest to compare maximum LBDFs produced for each girder for the series of tests that were studied. Therefore, numerical distribution factors for Section B-B were used to plot maximum distribution factors for all the tests from Table 3 and were compared to AASHTO factors from the 1993 guide specifications. Fig. 11 illustrates that maximum distribution factors for each girder determined from the

test truck locations from the numerical and modified AASHTO results produced similar trends except for Girder 5. Differences in trends for Girder 5 were attributed to the exclusion of parapets in the modified AASHTO procedure and the distance of Girder 5 away from the center of gravity of the test trucks. Including parapets in the calculation of modified AASHTO DFs would have increased deck stiffness over the exterior girders and thus created a more uniform distribution of the load; however, the simplified continuous beam model (Fig. 3) used to calculate DFs for the modified AASHTO procedure did not incorporate the additional stiffness. The 1993 AASHTO guide specification LBDFs were conservative for all girders, with levels of conservatism ranging from 10% for Girder 4 to 20% for Girder 3. As with the positive moment region, higher levels of conservatism were observed for Girders 1, 2, and 5 because of their distance from the centers of gravity of the test trucks.

Conclusions

The following conclusions can be drawn from this study:

1. Live-load lateral bending distribution factors calculated at the three radial cross sections in the positive moment region using the calibrated numerical model presented similar trends to factors calculated using modified AASHTO factors with differences on the order of 10–30%. When maximum values for each girder were examined the trends were identical for four of the five girders with only a 3–4% difference between factors;
2. The 1993 AASHTO guide specification LBDFs produced conservative factors when compared with test data from all of static tests at the examined radial cross sections. However, as expected, when maximum LBDFs from the numerical model and modified AASHTO procedure were compared to the 1993 AASHTO guide specification LBDF equation, resulting LBDFs were reasonably close with levels of conser-

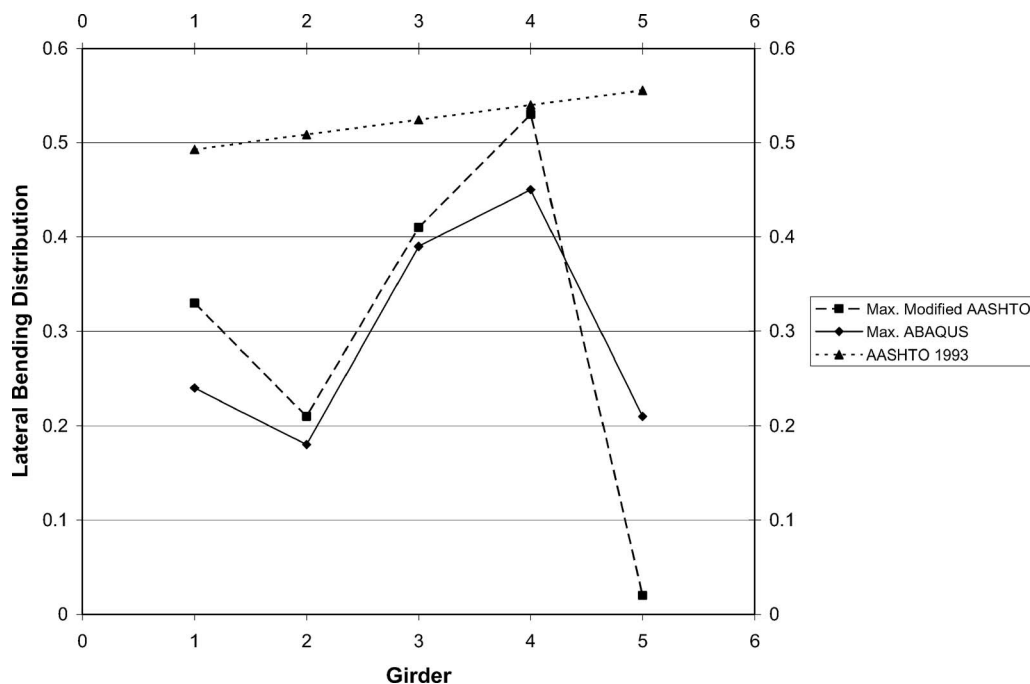


Fig. 11. Maximum live-load lateral bending distribution factors, Section B-B

vatism ranging from 8% for Girder 4 to 24% for Girder 3. Higher levels of conservatism were observed for Girders 1, 2, and 5 and were attributed to the relative distances of the centers of gravity of the test trucks from the girders in question;

- Live-load lateral bending distribution factors calculated in the negative bending moment region at Section D-D over Pier 2 using the numerical model presented similar trends to factors calculated using the modified AASHTO factors with differences on the order of 10–35%. Comparison between the maximum factors from each method produced similar trends, except for Girder 5, which indicated the girders closest to the centers of gravity of the test trucks produced the highest distribution factors. Differences were attributed to exclusion of parapets in the modified AASHTO procedures and the distance of Girder 5 from the centers of gravity of the test trucks; and
- The 1993 AASHTO guide specification LBDFs for three radial cross sections produced conservative LBDFs when compared with the calibrated numerical model for all of the static tests. However, when maximum LBDF values were compared, the 1993 AASHTO LBDF equation produced values that were reasonably close to numerical values for Girders 3 and 4 with differences ranging from 10% for Girder 3 to 20% for Girder 4. As with the three radial sections, Girders 1, 2, and 5 showed much higher levels of conservatism.

In conclusion, the 1993 AASHTO LBDF equation [Eq. (2)] conservatively predicts LBDFs with a level of conservatism, typically, between 20 and 30% for the field tested and modeled bridge discussed herein. The modified AASHTO procedure, which was developed exclusively for this study to facilitate accurate evaluation of LBDF equations for the field tests that were performed and involved adjusting the factor presented in Eq. (2) and used in Eq. (5) with Eq. (6), also produced conservative results near the test trucks' center of gravity but the level of conservatism was not as significant. From the results of this study the LBDF equation [Eq. (2)] presented in the 1993 guide specifications produces conser-

vative values that can be used for preliminary design and the initial sizing of girder flanges for this structure. While these results may be indicative of other structures, it is recommended that studies be completed to evaluate the parameters used in the 1993 guide specification LBDF equation for a wider range of parameters than those examined here.

Acknowledgments

The writers would like to acknowledge PennDOT and FHWA for providing assistance during the project.

Notation

The following symbols are used in this paper:

- DF_i = experimental and numerical live-load lateral bending distribution factors;
- DF_{Bi} = live-load distribution factor equations for lateral flange bending in each girder;
- L = span length (ft);
- M = lateral flange bending moment;
- M_s = equivalent straight girder major-axis bending moment;
- MF = modification factors that account for curvature;
- MF_{Bi} = modification factors for lateral bending moments;
- \bar{N} = $(R/100)(R > 100')$;
- R = radius [ft. ($R > 100'$)];
- R_i = reaction for any support i ;
- S = girder spacing [ft ($7' \leq S \leq 12'$)];
- σ_i = lateral bending stress for any member i along a selected radial section; and
- ΣP = sum of all wheel loads on the structure;
- $\Sigma \sigma$ = sum of all lateral bending stresses in all of the girders along the same radial section as σ_i .

References

- AASHTO. (1980). *Guide specifications for horizontally curved highway bridges*, AASHTO, Washington, D.C.
- AASHTO. (1993). *Guide specifications for horizontally curved highway bridges*, AASHTO, Washington, D.C.
- AASHTO. (2004). *LRFD bridge design specifications*, 3rd Ed., AASHTO, Washington, D.C.
- AASHTO. (2005). *LRFD bridge design specifications, 2005 Interim Revisions*, AASHTO, Washington, D.C.
- Bell, L. C., and Heins, C. P. (1970). "Analysis of curved bridges." *ASCE J. Struct. Div.*, 90(8), 1657–1673.
- Brockenbrough, R. L. (1986). "Distribution factors for curved I-girder bridges." *J. Struct. Eng.*, 112(10), 2200–2215.
- DePolo, D. S. (2004). "Evaluation of lateral flange bending for a horizontally curved I-girder bridge." MS thesis, Dept. of Civil and Environmental Engineering, The Pennsylvania State Univ., University Park, Pa.
- Galambos, T. V., Hajjar, J. F., Leon, R. T., Huang, W., Pulver, B. E., and Rudie, B. J. (1996). "Stresses in steel curved girder bridges." *Rep. No. MN/RC-96/28*, Minnesota Dept. of Transportation, Minneapolis.
- Hajjar, J. F., and Boyer, T. A. (1997). "Live-load stresses in steel curved girder bridges." *Progress Rep. on Task 1 Project 74708*, Minnesota Dept. of Transportation, Minneapolis.
- Heins, C. P., and Bonakdarpour, B. (1971). "Behavior of curved bridge models." *Public roads*, Vol. 36, Federal Highway Administration, Washington, D.C., 240–251.
- Heins, C. P., and Jin, J. O. (1984). "Live-load distribution on braced curved I-girders." *J. Struct. Eng.*, 110(3), 523–530.
- Heins, C. P., and Siminou, J. (1970). "Preliminary design of curved girder bridges." *Eng. J.*, 7(2), 50–61.
- Hibbitt, Karlsson, and Sorensen, (HKS). (2002). *ABAQUS/standard users manual: Version 6.3*, HKS, Providence, R.I.
- Krzmarzick, D. P., and Hajjar, J. F. (2006). "Load rating of composite steel curved I-girder bridges through load testing with heavy trucks." *Rep. No. MN/RC-2006-40*, Minnesota Dept. of Transportation, Minneapolis.
- Kulicki, J. M., Wassef, W. G., Kleinhans, D. D., Yoo, C. H., Nowak, A.S., and Grubb, M. (2006). "Development of LRFD specifications for horizontally curved steel girder bridges." *National Cooperative Highway Research Program Rep. 673*, Federal Highway Administration, Washington, D.C.
- Linzell, D. G., Laman, J. A., and Nevling, D. L. (2002). "Evaluation of level of analysis methodologies for horizontally curved I-girder bridges through comparison with measured response of an in-service structure—Instrumentation and field test plan." *Pennsylvania Transportation Institute Rep. No. 2002-32*, Pennsylvania Dept. of Transportation, Harrisburg, Pa.
- McElwain, B. A., and Laman, J. A. (2000). "Experimental verification of horizontally curved I-girder bridge behavior." *J. Bridge Eng.*, 5(4), 284–292.
- Nevling, D., Linzell, D., and Laman, J. (2006). "Examination of level of analysis accuracy for curved I-girder bridges through comparisons to field data." *J. Bridge Eng.*, 11(2), 160–168.
- United States Steel (USS). (1984). *V-load analysis*, National Steel Bridge Alliance, Chicago.